Mon. Not. R. Astron. Soc. **277**, 609–615 (1995)

A gravitational lens candidate behind the Fornax dwarf spheroidal galaxy

C. G. Tinney[1,2]★

[1] *Anglo-Australian Observatory, PO Box 296, Epping, NSW 2121, Australia*
[2] *European Southern Observatory, Garching bei München, Germany*

Accepted 1995 June 13. Received 1995 June 12; in original form 1995 April 19

ABSTRACT

We present observations of a candidate gravitational lens system behind the Fornax dwarf spheroidal galaxy, at $z = 1.406$ with a separation of 6.1 arcsec. The rest-frame velocity difference between the two components (from broad emission lines) is consistent with zero. The emission lines have similar strength in both components and show strong similarities. The continuum in component A, however, is ≈ 50 per cent brighter than in component B, and slightly bluer. The differences between the spectra can be accounted for by time-delay and/or microlensing effects, and the similarities between the spectra argue for a gravitational lens nature to the system.

Key words: Local Group – quasars: general – gravitational lensing.

1 INTRODUCTION

Advances in CCD astrometry have demonstrated the feasibility of milliarcsec precision relative astronomy at faint magnitudes (Tinney 1995), making the measurement of proper motions for the nearest galaxies a project requiring only years – not decades. A necessary prerequisite for such measurements, however, is a set of unresolved, extragalactic reference objects – i.e. QSOs. To identify such reference objects, Tinney et al. (1995, in preparation) have begun a search for the optical counterparts of *ROSAT* sources behind the nearest southern galaxies. CCD imaging in the *U* and *B* passbands enables UV-excess quasar candidates to be identified, and spectra are then obtained to check for the presence of emission lines. In the course of this programme, a pair of bright UV-excess candidates were identified behind the Fornax dwarf spheroid (dSph).

2 THE QSO PAIR

CCD images in the *U* (2700 s) and *B* (600 s) bands were acquired on 1994 October 27/28 (UT) with the Danish 1.54-m telescope at the European Southern Observatory, La Silla. The frames were centred on *ROSAT* sources from the list of Gizis, Mould & Djorgovski (1994). The images were photometered using a version of DoPHOT (Schecter, Mateo & Saha 1993) embedded in the FIGARO package, and calibrated by standards of Landolt (1992). A pair of strong UV-excess sources was found to be positionally coincident with Gizis et al.'s source 11. A 45 × 45 arcsec^2 portion of the *B*-band image containing these sources (labelled 'A' and 'B') is reproduced in Fig. 1, and the *B* and $U-B$ photometry for selected objects is presented in Table 1.

Preliminary spectroscopy of these objects was obtained on the ESO/MPI 2.2-m telescope with the EFOSC2 spectrograph on 1995 February 1/2 (UT). These data were poor, but did show C III] and Mg II lines in both A and B at $z \approx 1.4$. Further spectra were obtained with the 3.9-m Anglo-Australian Telescope (AAT) on 1995 March 3 (UT) using the RGO Spectrograph and Faint Object Red Spectrograph (FORS), in combination via a dichroic beam splitter. The RGO was used with the 250B grating in first order, positioned so as to give a wavelength coverage from 3300 Å to the dichroic cut-off at ≈ 5600 Å, at a resolution of 7 Å (1.7-arcsec slit) and a dispersion of 3.6 Å pixel^{-1}. FORS is a fixed-configuration grism spectrograph with a wavelength coverage from the dichroic cut-on at ≈ 5800 Å to 10 000 Å, at a resolution of 20 Å and a dispersion of 10.1 Å pixel^{-1}. Exposures totalling 3600 s were made on each spectrograph at a mean airmass of 1.67. Standard data reduction was carried out using the FIGARO package. The absolute wavelength calibrations are limited by flexure to ± 100 km s^{-1} for the RGO spectrograph and ± 400 km s^{-1} for FORS. Velocity differences, however, are more precisely determined: ± 14 km s^{-1} for the RGO spectrograph and ± 42 km

★ E-mail address: cgt@aaoepp.aao.gov.au

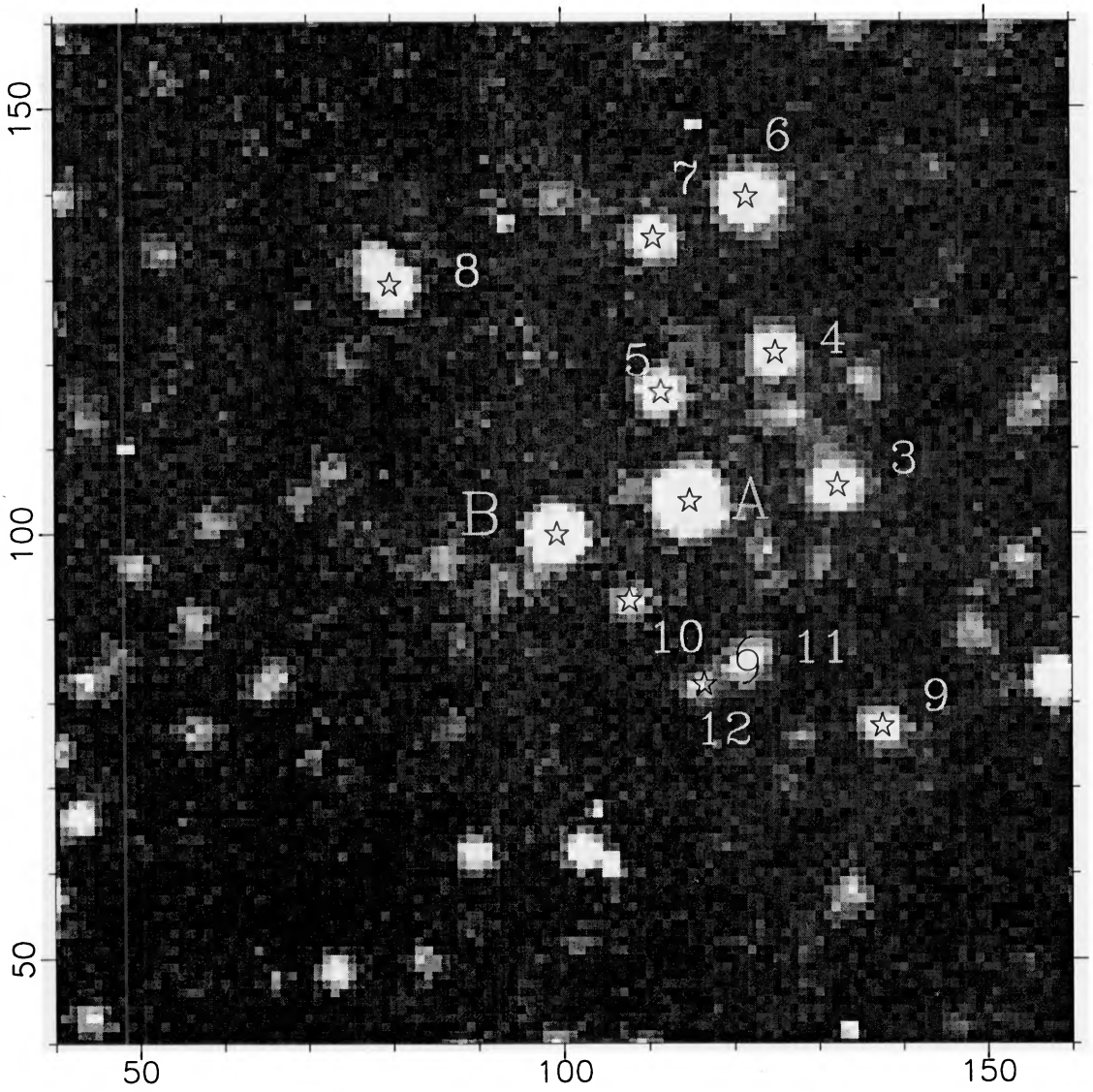

Figure 1. A 45×45 arcsec^2 *B*-band image in 1.5-arcsec seeing of the lens candidates. The axes are labelled in pixels – 1 pixel = 0.377 arcsec. North is to the top, and west to the left. Photometry for the marked objects is presented in Table 1.

s^{-1} for FORS. Flux calibration was carried out using the standard LTT 1788 of Baldwin & Stone (1984), and atmospheric absorption was corrected using a smooth-spectrum star.

Fig. 3 shows the spectra derived for each of the components A and B. The line parameters obtained by Gaussian fits to the continuum-subtracted spectra (see Section 3.2) are given in Table 2. Fig. 3 also shows evidence for at least one, and possibly two, absorption systems – the specific lines identified are given in Table 3. Mg II, Mg I and Fe II lines are seen at $z \approx 0.54$ in both components ($\overline{z} = 0.5431 \pm 0.0003$ in A, $\overline{z} = 0.542 \pm 0.001$ in B). There is also evidence to suggest that several of the same lines are seen at a redshift of $z = 0.338 \pm 0.001$ in component A, where the Mg II doublet falls on the red wing of the C IV line.

Infrared data were obtained on the AAT using the IRIS camera at *H* band on the night of 1995 March 13 (UT). 36 offset 60-s exposures were taken in the *f*/36 'wide' mode, which has a pixel scale of 0.79 arcsec pixel^{-1}, and later mosaicked. The final seeing of this resampled frame was 1.1 arcsec. This image (see Fig. 2) was also photometered using DoPHOT, and the resulting *H* photometry is shown in Table 1.

The position of component A is $02^h40^m07^s.73$, $-34°34'19''.8$ (J2000.0), as obtained from COSMOS scans of the UKST Southern Sky Survey (Yentis et al. 1992). The QSO pair is hereafter QJ0240−343AB. No radio source was found at the position of the pair to a level of ~1 mJy (21-cm continuum) in the NRAO VLA Sky Survey (Condon et al. 1994).

3 A GRAVITATIONAL LENS?

Recent reviews (e.g. Blandford & Narayan 1992; Schneider, Ehlers & Falco 1992) have highlighted the fact that a number of criteria need to be fulfilled before a candidate becomes a 'secure' gravitational lens (GL): the redshifts should agree to high tolerances (ideally to better than 50 km s^{-1}; Schneider et al. 1992); the components should show significant spectral

similarities; and lastly, some form of lensing object should be detectable. However, there are pitfalls: microlensing by stars in a lens can modify the equivalent widths and redshifts of broad emission lines – only narrow lines can place stringent limits on velocity differences; both microlensing and time-delay can modify the line-to-continuum ratios of lensed images; and several accepted GL systems exist in which no lens has yet been unambiguously detected (e.g., Q2345+007, Q1635+267). With this mind, do the data obtained contradict the hypothesis that this pair is a GL?

3.1 Photometry of the QSOs

The *observed* absolute magnitudes of the QSO pair are $M_{B,A} = -26.8$, $M_{B,B} = -26.1$ ($H_0 = 50$ km s^{-1} Mpc^{-1}, $q_0 = 0.5$, k-correction due to Cristiani & Vio 1990). If the system is a GL, however, the images will have been amplified by factors which depend strongly on the specific geometry of the QSO and lens.

Component B has a $B-H$ colour 0.50 mag redder than component A, and a redder optical continuum (Section 3.2).

Table 1. Position and magnitude information.

Obj	X,Y[a]	B	U-B	B-H	Cl[b]
		DoPHOT Photometry			
A	114.9,103.7	19.00±0.05	-1.02±0.08	1.42±0.08	s
B	99.3,99.9	19.77±0.05	-1.09±0.08	1.92±0.08	s
3	132.3,105.6	20.51±0.06	0.27±0.10	2.98±0.08	s
4	125.0,121.2	20.40±0.06	0.75±0.12	3.34±0.08	s
5	111.5,116.6	20.60±0.06	0.94±0.15	3.81±0.08	s
6	121.6,139.6	19.71±0.05	0.24±0.08	2.11±0.08	ns
7	110.7,134.8	20.70±0.06	0.46±0.11	3.47±0.08	s
8	79.8,129.3	20.41±0.06	$\gtrsim 0.4$	4.10±0.08	s
9	137.5,77.2	21.13±0.06	0.09±0.12	2.88±0.09	ns
10	107.8,92.0	21.65±0.07	0.12±0.15	2.60±0.09	s
11	121.6,84.8	20.91±0.06	0.49±0.14	2.51±0.09	ns
12	116.5,82.1	21.92±0.09	-0.32±0.17	–	?
		Aperture Photometry[c]			
G1	108,105	22.7±0.2		20.9±0.2	?
G2	107,110	24±0.5		21.1±0.2	?
G3	120,110	22.8±0.2		20.2±0.2	?
G4	93,94	21.6±0.2		20.4±0.2	?
G5	86,97	21.4±0.2		20.0±0.2	?

[a]0.377 arcsec pixel^{-1}. X increases to the west; Y increases to the north.
[b]DoPHOT classification; s = star, ns = non-stellar, ? = unclassified.
[c]Photometry of 'galaxies' (in a 2.6-arcsec aperture) after DoPHOT subtraction of stellar objects.

If the $B-H$ colours are treated as measures of the spectral index for the components, α, (where $F_\nu \propto \nu^\alpha$), then we obtain $\alpha_A = 0.1$, $\alpha_B = -0.2$. If the system is a GL, however, this colour difference could be due to reddening by a foreground galaxy, or to the contribution of 'extra' light from an underlying red source (e.g. a galaxy), or to an intrinsic variation in the QSO continuum seen in one component and/or pass-band, due to the lens time-delay.

The $B-H$ colour difference corresponds to a small extinction difference between the lines of sight. The actual value depends on the redshift at which the reddening is assumed to take place – in the observed frame it corresponds to $\Delta A_V \approx 0.44$; for $z \approx 0.5$, $\Delta A_V \approx 0.31$; and for reddening near the QSO ($z \approx 1.4$), $\Delta A_V \approx 0.18$. These values are so small (unlike, for example, Q1009−0252; Hewett et al. 1995) that they place no real limit on the observability of the source of the extinction. (Reddening in the Fornax dSph is unlikely – no ISM is known in any of the Milky Way dSphs.) Underlying galaxies in the redder component of GL candidates have been seen in several cases (e.g. Surdej et al. 1988; Turner et al. 1988). Similar techniques have been used on these data, but there is no evidence for an underlying galaxy – a limit of $R \sim 20$ can be placed on the presence of a lens underlying component B. Lastly, the colour difference can be explained by variability in the QSO continuum, when combined with the expected light-travel delay (~1.5 yr; Schneider et al. 1992), and the 4-month time difference between the B and H data. As an example, Sitko et al. (1993) observe changes of 0.0–0.5 mag on year-long time-scales in the $U-I$ colour of PG 1202+281 ($M_B \sim -24.5$), which, at $z = 0.165$, corresponds to $B-H$ at $z = 1.4$.

Table 3. Absorption-line identifications and wavelengths.

		QJ0240-343 A			QJ0240-343 B		
ID	λ_{rest} (Å)	λ_{obs} (Å)	EW (Å)	z	λ_{obs} (Å)	EW (Å)	z
FeII	2382	3675	1.0	0.5430	3671	0.4	0.541
FeII	2586	3991	1.9	0.5434	–		
FeII	2600	4011	1.3	0.5427	4013	1.5	0.543
MgII	2796	4315	2.1	0.5432	4310	1.9	0.542
MgII	2803	4325	2.9	0.5430	4324	3.4	0.543
MgI	2852	4402	1.2	0.5434	4400	1.1	0.543
FeII	2600	3479	5.0	0.3382	–		
MgII	2796	3745	3.2	0.3390	–		
MgII	2803	3755	2.5	0.3394	–		
MgI	2852	3811	2.6	0.3363	–		

Table 2. Emission-line identifications and parameters.

		QJ0240-343 A				QJ0240-343 B				
ID	λ_{rest} (Å)	λ_{obs} (Å)	FWHM[a] (Å)	Line Flux[b] (mJy Å)	z	λ_{obs} (Å)	FWHM[a] (Å)	Line Flux[b] (mJy Å)	z	v_{obs}(A − B) (km/s)
CIV	1549	3710±2	84	2.5	1.395±0.002	3725±2	75	1.9	1.405±0.002	1210
AlIII	1858	4478±2	39	0.57	1.410±0.002	4478±2	48	0.34	1.410±0.002	0
CIII]	1909	4577±2	95	2.4	1.398±0.002	4588±2	100	1.9	1.403±0.002	720
MgII[c]	2798	6753±5	85	4.2	1.414±0.002	6763±5	83	3.0	1.417±0.002	440

[a]FWHM values ±15 per cent. [b]Line fluxes ±10 per cent. [c]Because of underlying emission, only the line core is fitted.

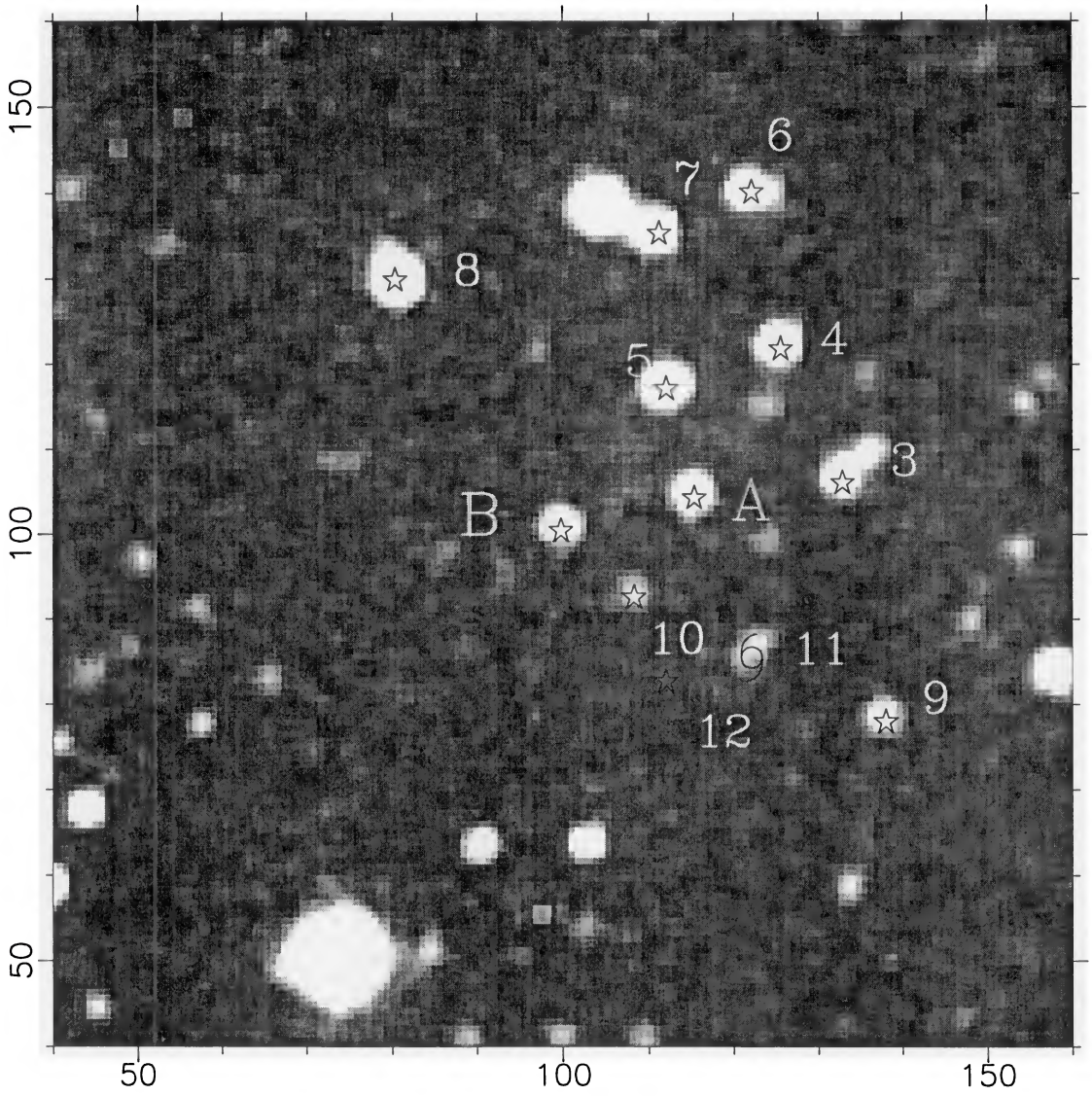

Figure 2. Same as Fig. 1 in the *H*-band (1.1-arcsec seeing).

3.2 Spectra of the QSOs

The mean difference in rest-frame velocity of the two components (cf. Table 2) is 250 ± 180 km s^{-1} – i.e. consistent with zero. Cross-correlation of the two spectra produces little more information than this. Once regions of the spectra dominated by absorption-line systems, night-sky lines and terrestrial absorption are removed, only the broad emission lines are left. These give rest-frame velocity differences consistent with zero at uncertainties of ≈ 200 km s^{-1}.

Assigning 'underlying' continua to QSO spectra is problematic at best (Francis et al. 1991). Based on the composite QSO spectra of Boyle (1990) and Francis et al., three regions in the observed wavelength range can be expected to approximate the continuum: $\lambda_{\rm rest} = 1440$–$1480$, 2175–2225 and 3000–3050 Å. The mean ratio for the continua in these regions is $(\mathrm{A/B})_{\rm cont} = 2.00 \pm 0.2$ (the uncertainty reflects the observed ratio range), with the ratios being smaller at longer wavelengths. Line spectra were constructed by subtracting a low-order polynomial fitted through these continuum regions (see Fig. 3). Straight means of the flux in the line spectra in ranges containing the emission lines, and Gaussian fits to the line spectra, give ratios for the line fluxes which are slightly different, but (considering the difficulty of selecting continua in the absence of an a priori model) consistent with a single multiplicative factor of $(\mathrm{A/B})_{\rm line} = 1.3 \pm 0.2$. Therefore $(\mathrm{A/B})_{\rm cont} \neq (\mathrm{A/B})_{\rm line}$ – the continuum in component A is at least 50 per cent brighter than in component B.

This can be foreseen under the GL hypothesis in two ways. The difference could be due to microlensing by stars in the lens if it overlies the light path to image A. Such microlensing will preferentially magnify the small continuum region at the centre of a QSO, producing the observed line-to-continuum difference. This interpretation is supported by the fact that the metal-line absorption systems at $z = 0.543$ and 0.339 – assuming that they can be associated with a lensing galaxy – are stronger in A. However, the 'reddening' of B would then require another object along its line of sight. Unfortunately, the confirmation of this mechanism by

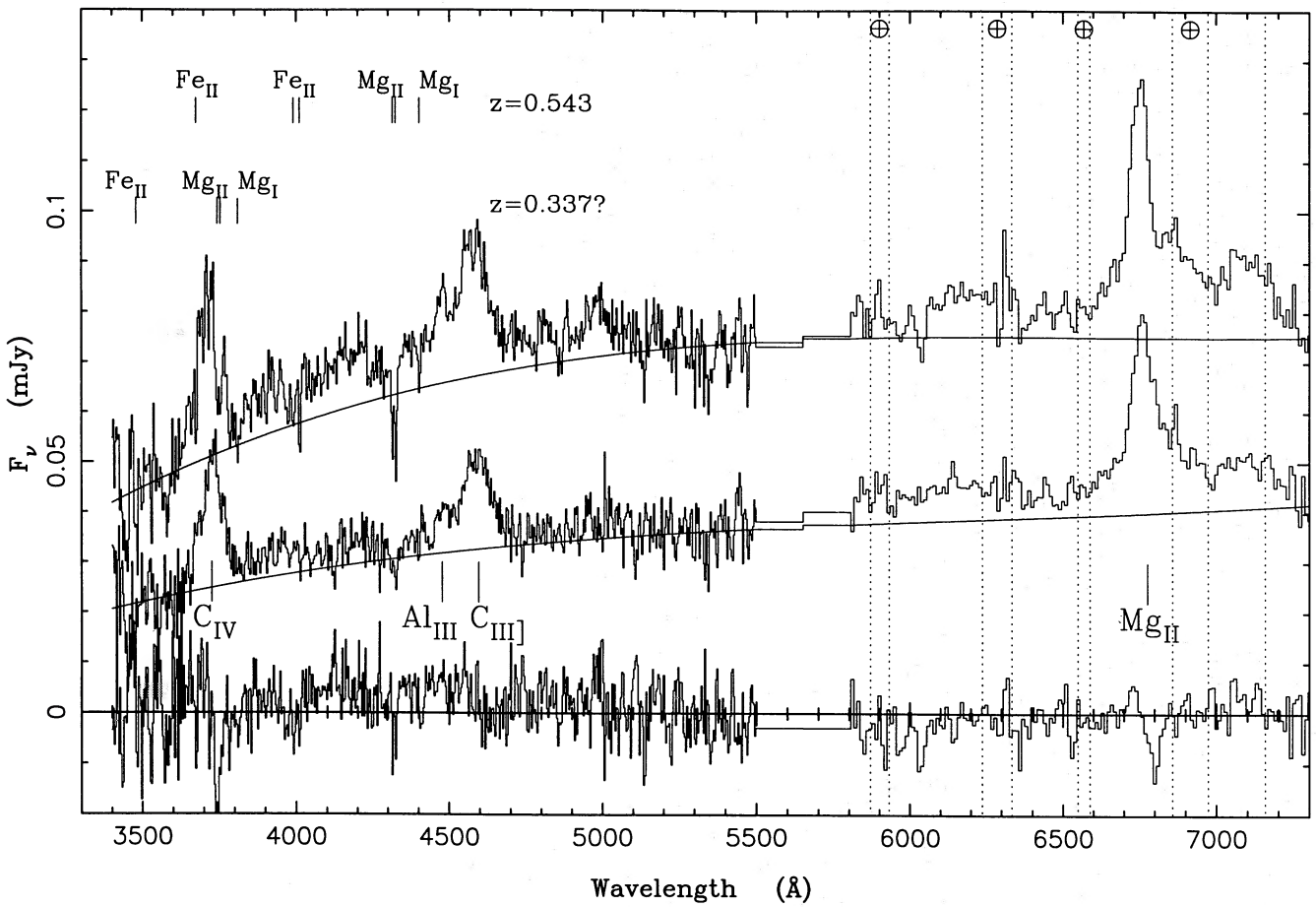

Figure 3. Spectra obtained with the 3.9-m AAT and RGO+FORS of QJ0240−343A (upper trace) and QJ0240343B (middle trace). The difference between the line spectra (lower trace) is described in Section 3.2. The regions where terrestrial water vapour is not well corrected are marked.

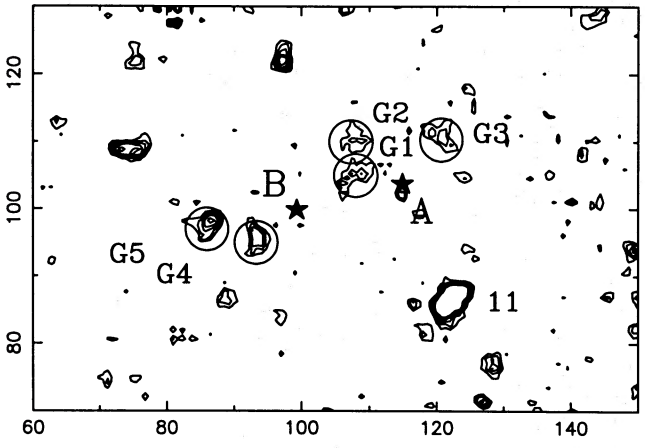

Figure 4. Expanded *H*-band image after removal of stellar images (cf. Section 3.3. There are five contours between 1.5 and 4σ per pixel).

monitoring will be problematic – the time-scales for microlensing at cosmological distances are quite long (e.g. ~8 yr for a 0.1 $M_\odot$ microlens with $v_t = 480$ km s^{-1} at $z = 0.54$, or ~25 yr for a similar 1-$M_\odot$ microlens; Blandford & Narayan 1992).

Alternatively, variability in the continuum luminosity of the QSO will take a finite time (τ_{BLR}) to 'propagate' to the broad-line region (BLR). Following Peterson (1993), a QSO with an intrinsic luminosity $M_B \sim -25$ to -26 would be expected to show $\tau_{BLR} \sim 3$–5 month. As changes in the QSO should be observed with a ~1.5-yr light-travel lag between the images, it is foreseeable that at a particular epoch, a change in the QSO continuum is not seen in the broad lines. Such an argument, however, relies on a relatively small magnification of the primary (i.e., less than a factor of 5). If the geometry for the lens is such that the magnification is more extreme, say a factor of 40 or more, then the intrinsic luminosity would be more like $M_B \sim -21$ to -22, implying a $\tau_{BLR} \lesssim 20$ d. The observed line-to-continuum ratios would then require that the observations were made at a very special time, thus arguing against this mechanism. Resolution of this issue will await the firm detection of lens candidates and detailed modelling. However, *if* this mechanism is at work in QJ0240−343AB, then spectral monitoring will strongly test the GL hypothesis, since the QSO continuum must vary by ~50 per cent with a light-travel delay, while changes in the line-to-continuum ratios must reflect both the light-travel delay *and* τ_{BLR}. [Because the available scans of archival UKST plates are confused in the region, they provide little useful data. The COSMOS scans show

QJ0240−343A, but B is confused. The APM scans show the entire region confused. Visual inspection of the two UKST *J* survey plates covering the Fornax dSph (epochs of 1979 August 23 and November 16) show QJ0240−343A brighter than B, although the magnitude difference appears to be less than that observed in 1994/5.]

Fig. 3 also shows the difference between the line spectra in the sense A−1.3×B. Apart from the Mg II line in B being shifted to the red relative to A, and the presence of absorption on the red wing of the C IV line in A, the two line spectra show similar shapes and widths – as indicated by the fitted parameters of Table 2. If we ignore GL candidates whose status is unclear, the number of close QSO pairs currently known is quite small (Djorgovski 1991). There are only three at arcsec-scale separations with velocity differences less than 1000 km s^{-1} – although if we include 'unfashionable' GL candidates the number may be more like six. In almost all cases, the spectra of such *bona fide* QSO pairs (e.g. Q1343+164, Crampton et al. 1988; Q1145−071, Djorgovski et al. 1987; Q0151+048, Meylan et al. 1990) show discrepancies much more significant than those seen in Fig. 3. The differences which *are* seen are not sufficient to rule out a GL nature (see, e.g., Steidel & Sargent 1991). Given the combination of circumstances that (1) the spectra are sufficiently similar that their differences can be accounted for by microlensing and/or time-delay effects, but (2) not as discrepant as the known *bona fide* QSO pairs, the GL hypothesis is considerably strengthened.

3.3 Imaging

The photometry of Table 1 indicates that no other object in the field shows colours similar to those of QJ0240−343A,B – i.e., there is no evidence for further lensed images brighter than $B \approx 21$. QJ0240−343AB (like the other wide, separation GL candidates) requires a massive lens to achieve an image separation of 6.1 arcsec – a simple point-mass model, at the redshift of the strongest Mg II absorption system, would require a mass of $\approx 2.0 \times 10^{12}\ M_{\odot}$ interior to the QSO images (Blandford & Narayan 1992). Alternatively, a singular isothermal sphere model would require a lensing galaxy with a velocity dispersion of $\sigma \approx 480$ km s^{-1}. Both estimates would place such a lens in the realm of the most massive and brightest galaxies known. In comparison, the brightest cluster elliptical (BCE) lens in Q0957+561 has $\sigma \approx 390$ km s^{-1} and $R = 17.0$ at $z = 0.35$ (Falco, Gorenstein & Shapiro 1991; Bernstein, Tyson & Kochanek 1993).

As noted above, the spectra place a limit of $R \sim 20$ for a galaxy underlying component B – does the imaging data show any evidence for a massive lens? Fig. 4 shows the *H*-band data after the sources classified by DoPHOT as 'stellar' have been removed from the frame. Aperture photometry of these faint 'non-stellar' objects in a circle of 10-arcsec radius centred on QJ0240−343A is shown in Table 1. It should be noted, however, that these 'galaxies' may be chance arrangements of faint stars in the Fornax dSph, rather than real galaxies. The point to note is that no bright galaxies are seen between the components. The brightest galaxy in the vicinity of the system is object '11' (7.6 arcsec to the SW of component A, with $H = 18.6$ and $B - H = 2.4$), which is significantly fainter than the Q0957+561 BCE. The absence of such an easily detected galaxy near the QJ0240−343AB joining line rule out a single massive and luminous galaxy as a lens. The only galaxy which *is* seen to lie 'between' the two QSO images is G1 ($H = 20.9$). The absence of an obvious lens points to either a dark lensing component, as has been suggested in Q2345+007AB, Q1635+267 and Q1429−008AB (e.g. Hewett et al. 1989; Narashima & Chitre 1989; McLeod, Rieke & Weedman 1994), or the presence of a cluster which 'aids' lensing by G1, as in the case in Q0957+561, and has been suggested in Q2345+007AB by Fischer et al. (1994). In a region of diameter 30 arcsec, three 'galaxies' of magnitude similar to object 11 are seen at *H*, while the number of fainter G1–5 type 'galaxies' is almost 15. Such data are by no means conclusive, but hint at the possible presence of a cluster at magnitudes consistent with a redshift of $z \sim 0.3$–0.5. However, because of the dSph stars in the foreground, confirmation of the existence of a cluster will require deep imaging in exceptionally good seeing, followed by spectroscopy of the possible cluster members.

4 CONCLUSION

Observations of a wide-separation GL candidate behind the Fornax dSph galaxy have been obtained. The spectroscopic and photometric data obtained to date strongly suggest that the system is a GL, but cannot rule out the possibility that the system is a QSO pair. No evidence is seen for a convincing lensing mass in our imaging data, although Mg II absorption systems are seen in the QSO spectra at $z \sim 0.543$ and 0.338. If QJ0240−343AB is a GL, then the lensing mass may have a dark component. The imaging data hint at the possible existence of a cluster. The large difference in the line-to-continuum ratios suggests that if the system is a lens, then the lensed QSO may be quite variable.

ACKNOWLEDGMENTS

I thank G. Da Costa, S. Lumsden and J. Spyromilio for assistance at the AAT, G. Robertson and an anonymous referee for comments on an earlier version of this paper, and the COSMOS, APM and UKST units for providing plate data. Observations were made at the European Southern Observatory, La Silla, Chile and the Anglo-Australian Telescope, Mt. Sidings Springs, Australia.

REFERENCES

Baldwin J. A., Stone R. P. S., 1984, MNRAS, 206, 241
Bernstein G. M., Tyson J. A., Kochanek C. S., 1993, AJ, 105, 816
Blandford R. D., Narayan R., 1992, ARA&A, 30, 311
Boyle B. J., 1990, MNRAS, 243, 231
Condon J. J. et al., 1994, PASP, submitted
Crampton D. et al., 1988, ApJ, 330, 184
Cristiani S., Vio R., 1990, A&A, 227, 385
Djorgovski S. G., 1991, in Crampton D., ed., ASP Conf. Ser. Vol. 21, The Space Distribution of Quasars. Astron. Soc. Pac., San Francisco, p. 349
Djorgovski S. G., Perley R., Meylan G., McCarthy P., 1987, ApJ, 321, L17
Falco E. E., Gorenstein M. V., Shapiro I. I., 1991, ApJ, 372, 364
Fischer P. E., Tyson J. A., Bernstein G. M., Guhathakutra P., 1994, ApJ, 431, L71
Francis P. J. et al., 1991, ApJ, 373, 465
Gizis J. E., Mould J. R., Djorgovski S., 1993, PASP, 105, 871
Hewett P. C. et al., 1989, ApJ, 346, L61

Hewett P. C. et al., 1994, AJ, 108, 1534
Landolt A. U., 1992, AJ, 104, 340
McLeod B., Rieke M., Weedman D., 1994, ApJ, 433, 528
Meylan G., Djorgovski S., Weir N., Shaver P., 1990, ESO Messenger, 59, 47
Narashima D., Chitre S. M., 1989, AJ, 97, 327
Peterson B. M., 1993, PASP, 105, 247
Schecter P. L., Mateo M., Saha A., 1993, PASP, 105, 1324
Schneider P., Ehlers J., Falco E. E., 1992, Gravitational Lenses. Springer-Verlag, New York, p. 43
Sitko M. L., Sitko A. K., Siemiginowska A., Szczerba R., 1993, ApJ, 409, 139
Steidel C. C., Sargent W. L. W., 1991, AJ, 102, 1610
Surdej J. et al., 1988, Nat, 329, 695
Tinney C. G., 1995, in Walsh J. R., ed., Science with the VLT. Springer-Verlag, Heidelberg
Turner E. L., Hillenbrand L. A., Schneider D. P., Hewitt J. A., Burke B. F., 1988, AJ, 96, 1682
Yentis D. J. et al., 1992, in MacGillivray H., Thomson E., eds, Digitised Optical Sky Surveys. Kluwer, Dordrecht, p. 67